

Field monitoring of boundary layer wind characteristics in urban area

Q.S. Li^{1*}, Lunhai Zhi^{1,2} and Fei Hu³

¹Department of Building and Construction, City University of Hong Kong, Tat Chee Avenue, Kowloon, Hong Kong

²College of Civil Engineering, Hunan University, Changsha, Hunan 410082, PR China

³Institute of Atmospheric Physics, Chinese Academy of Sciences, Beijing 100029, PR China

(Received December 8, 2008, Accepted August 24, 2009)

Abstract. This paper presents statistical analysis results of wind speed and atmospheric turbulence data measured from more than 30 anemometers installed at 15 different height levels on 325 m high Beijing Meteorological Tower and is primarily intended to provide useful information on boundary layer wind characteristics for wind-resistant design of tall buildings and high-rise structures. Profiles of mean wind speed are presented based on the field measurements and are compared with empirical models' predictions. Relevant parameters of atmospheric boundary layer at urban terrain are determined from the measured wind speed profiles. Furthermore, wind velocity data in longitudinal, lateral and vertical directions, which were recorded from an ultrasonic anemometer during windstorms, are analyzed and discussed. Atmospheric turbulence information such as turbulence intensity, gust factor, turbulence integral length scale and power spectral densities of the three-dimensional fluctuating wind velocity are presented and used to evaluate the adequacy of existing theoretical and empirical models. The objective of this study is to investigate the profiles of mean wind speed and atmospheric turbulence characteristics over a typical urban area

Keywords: field measurement; boundary layer wind characteristic; wind speed profile; atmospheric turbulence; tall building design.

1. Introduction

Field measurements of wind characteristics and atmospheric turbulences are very useful, particularly for further understanding wind climates, for calibrating codes of practice for wind-resistant design of structures and for incorporation into useable wind tunnel simulations and numerical modeling. It has been recognized that field measurement is the most reliable tool for investigation of wind characteristics in the atmospheric boundary layer (ABL).

Determination of the vertical distributions of wind speed in the ABL over various types of surface terrains is necessary, since such information is essential for the wind-resistant design of tall buildings, wind tunnel simulations and numerical modeling. There have been a number of studies that used wind data from various elevations at towers for evaluation of wind speed profiles (Thuillier and Lappe 1964, Panofsky and Petersen 1972, Carl, *et al.* 1973, Korrell, *et al.* 1982,

* Corresponding Author, E-mail: bcqsl@cityu.edu.hk

Holtslag 1984, Karlsson 1986, Grant 1994, Holmes, *et al.* 1997, Holmes 2007, Tieleman 2008, etc). These studies provided very useful information on the boundary layer wind characteristics over various terrain conditions. Recently, Doppler sodar was employed to measure mean wind speed profiles, which is an effective tool to investigate the vertical distributions of wind speed characteristics (Thomas and Vogt 1993, Vogt and Thomas 1995, Tamura, *et al.* 2001, 2007, etc). However, reliable field measurements of mean wind speed profiles and atmospheric turbulence characteristics in boundary layers over urban areas are still very limited. Hence, it is necessary to collect such information. In this regard, a comprehensive field measurement program has been conducted for investigating the boundary layer wind characteristics over a typical urban area in Beijing, which involves more than 30 anemometers installed at 15 different height levels on the Beijing Meteorological Tower with height of 325 m from the ground. Significant field data have been measured from the instrumented tower over the last several years, including measurements made during a number of windstorms. This paper presents selected results from the analysis of the measured data from numerous anemometers installed at 15 different height levels on the Beijing Meteorological Tower, including the profiles of mean wind speed and atmospheric turbulence information.

The wind flow in the atmospheric surface layer is highly turbulent, and the wind loads acting on buildings and structures are significantly influenced by the approaching turbulent flow characteristics. Extensive field measurement studies on atmospheric turbulence characteristics have been conducted in the past. Significant efforts have been made to investigate wind speed spectra and turbulence characteristics based on measurements from numerous heights at various sites and to define their general behavior in terms of similarity parameters. Several spectra forms have been proposed, which are of course essential for developing a suitable description and understanding of nature of fluctuating wind velocities (von Karman 1948, Davenport 1961, Kaimal, *et al.* 1972, Panofsky, *et al.* 1959, 1982, Olesen, *et al.* 1984, Solari and Piccardo 2001, Shiau and Chen 2002, etc). The parameters of turbulent flow such as gust factor, turbulence intensity and turbulence integral length scale were also obtained from numerous studies aiming at investigating the basic physics of wind flows (von Karman 1948, Panofsky, *et al.* 1977, Grag, *et al.* 1997, Roth 2000, Shiau and Chen 2002, Li, *et al.* 2003, 2004a, 2004b, 2005, Eliasson, *et al.* 2006, Cheng, *et al.* 2007, Tamura, *et al.* 2001, 2007, Holmes, *et al.* 1997, Law, *et al.* 2006, Holmes, *et al.* 2005, Holmes 2007, Schroeder, *et al.* 2009, etc). However, literature review reveals that the information obtained in the previous studies mostly concern atmospheric turbulence and wind speed profiles over relatively smooth and homogeneous surfaces. There is considerable uncertainty and lacking of information about wind structures over city terrains, although more and more high-rise structures have been or are being built in urban areas throughout the world. Therefore, there is an urgent need to conduct such studies.

In this study, data measured from numerous anemometers installed at 15 different heights on the 325 m Beijing Meteorological Tower (shown in Figs. 1 and 2) during several windstorms in 2002 and 2003, were analyzed and discussed. The wind speed profiles and atmospheric turbulence characteristics over a typical urban area, including distributions of mean wind speed and mean wind direction, roughness length, zero-plane displacement, surface friction velocity, height of ABL, turbulence intensity, gust factor, turbulence integral length scale, power spectral density, etc. are investigated in detail. Moreover, their variations with mean wind speed are also discussed. The main objective of this study is to further the understanding of wind speed profiles and atmospheric turbulence characteristics over a typical urban area and provide useful information on the wind-resistant design of tall buildings and high-rise structures.

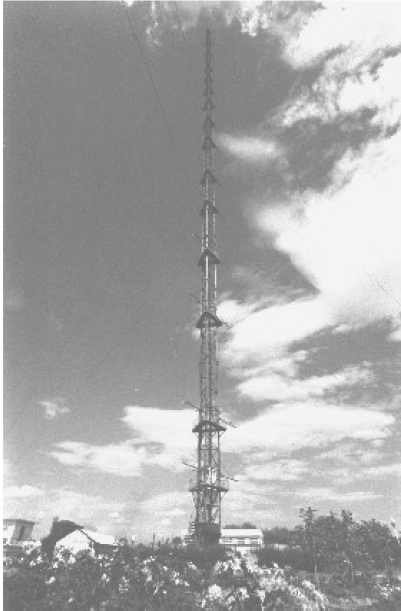


Fig. 1 Beijing Meteorological Tower

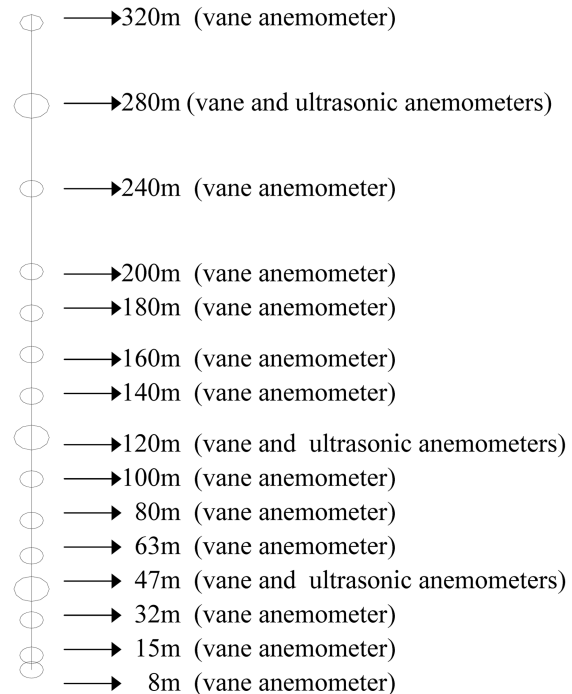


Fig. 2 Anemometer locations in Beijing Meteorological Tower

2. Introductions of the field measurement arrangements

The Beijing Meteorological Tower, which has a height of 325 m, is located in north central Beijing. The height of its base is about 48.63 m above the sea level and is located at 39°58'N, 116°22'E. When it was built nearly three decades ago, the land within a radius of 1000 m from the tower was flat with low-rise buildings (3~5 stories in height). Fig. 1 shows a photo of the tower at that time. With the development of urbanization in Beijing over the past two decades, the tower site is now surrounded by a number of tall buildings including several 60 m high buildings located 300 m away in the Southern direction. Towards the north some tall buildings with heights of 70~90 m are about 500 m away from the tower location. There are some low-rise houses and trees to the east of the tower. The west of the tower corresponds to the area covered by a mixture of trees, low-rise residential houses (about 7~25 m high) and tall buildings (about 40 m in height) (Al-Jiboori and Hu 2005). The site around the tower can be regarded as terrain C (an urban area) according to the Chinese National Load Code (GB50009-2001). Thirty vane anemometers (EC9-1 with high resolution (0.1 m/s) made by Changchun Meteorological Instrument Research Institute, China) were installed on the tower at fifteen levels with heights of 8 m, 15 m, 32 m, 47 m, 63 m, 80 m, 100 m, 120 m, 140 m, 160 m, 180 m, 200 m, 240 m, 280 m and 320 m, respectively to measure mean wind speed data at a sample rate of 0.05 Hz (see Fig. 2). In addition, three ultrasonic anemometers (made by Institute of Atmospheric Physics, Chinese Academy of Sciences) were mounted at the 47 m, 120 m and 280 m high levels to record three-dimensional mean and fluctuating wind velocity with sampling rate of 10 Hz. The mean wind speed data measured by the

Table 1 Information on the field measurement results presented in this paper

Name of windstorm	Date	Wind direction	Wind speed record length (minutes)	Maximum Peak Gust (m/s)
“0320”(15 levels)	20 th March 2002	NW	840	31(at 320 m height)
“0218”(47 m height)	18 th February 2003	NE	1020	23.8
“0419”(47 m height)	19 th April 2003	NE	480	27.3

thirty vane anemometers on 20th March 2002 was used in this paper to evaluate the vertical distributions of mean wind speed in the atmospheric boundary layer. Meanwhile, the wind velocity data recorded from the ultrasonic anemometer at 47 m height on the tower were analyzed for investigating 3D atmospheric turbulence characteristics, which were measured during the passages of three windstorms in 2002 and 2003. Table 1 presents the relevant information on the windstorms.

3. Empirical models of wind speed profile

As reviewed previously, there have been several theoretical and empirical models such as log law, power law and Deaves-Harris model (D-H model) available for describing vertical distributions of mean wind speed in the atmospheric boundary layer.

3.1. Log law

According to the asymptotic similarity considerations for a neutral atmospheric boundary layer, the wind speed profile can be expressed as:

$$U(z) = \left(\frac{U_0^*}{\kappa} \right) \ln \left(\frac{z}{z_0} \right) \quad (1)$$

where $U(z)$ is the mean wind speed at height z ; U_0^* is surface friction velocity; κ is von Karman's constant (here assumed to be 0.4); z_0 is surface roughness length. In addition, to take into account the fact that for a dense canopy of surface-covering objects such as buildings and vegetations, the mean flow does not necessarily penetrate downward to the very bottom of the roughness layer ($z=0$). Eq. (1) is corrected by displacing the vertical axis origin (William and Wilfried 1986, Wieringa 1993, Holmes 2007, Zilitinkevich, *et al.* 2008):

$$U(z) = \left(\frac{U_0^*}{\kappa} \right) \ln \left(\frac{z - z_d}{z_0} \right) \quad (2)$$

where z_d is the zero-plane displacement.

3.2 Power law

For the assessment of wind loads on structures, the power law profile has been used most widely because of its simplicity (Davenport 1960). It can be written as:

$$\text{Power law: } \frac{U(z)}{U(z_{ref})} = \left(\frac{z}{z_{ref}} \right)^a \quad (3)$$

where $U(z_{ref})$ is the mean wind speed at the reference height z_{ref} ; α is ground roughness exponent. The power law wind profile is entirely empirical and was developed without much reference to the real physics of atmospheric boundary layer. It has been adopted in several wind or structural design standards such as the building design codes of China, Japan and USA. In the current version of the Chinese National Load Code (GB50009-2001), the 10-minute mean wind speed at 10 m height is adopted as the reference wind speed. For urban terrain (category C) such as the instrumented tower site, the ground roughness exponent α is 0.22.

3.3. Deaves and Harris model (D-H mode)

The Deaves-Harris model includes three parameters z_0 , U_0^* and h and incorporates more of the real physics of atmospheric boundary layer. It will be applicable to the entire atmospheric boundary layer, and is not limited to the surface layer. The model is expressed as (Deaves 1981a, 1981b):

$$\frac{U(z)}{U_0^*} = \frac{1}{k} \left\{ \ln\left(\frac{z}{z_0}\right) + 5.75\frac{z}{h} - 1.88\left(\frac{z}{h}\right)^2 - 1.33\left(\frac{z}{h}\right)^3 + 0.25\left(\frac{z}{h}\right)^4 \right\} \quad (4)$$

where h is the height of atmospheric boundary layer which, according to the model, is determined by:

$$h = \frac{U_0^*}{Bf} \quad (5)$$

in which B is empirical constant and its magnitudes based on observed wind profiles is 6; f is Coriolis parameters ($9.375 \times 10^{-5} \text{ s}^{-1}$).

4. Mean wind speed distributions

The mean wind speed and wind direction measured by the thirty vane anemometers at the 15 levels during a windstorm on 20th March 2002 (“0230”) were analyzed by averaging the data over 10min. Fig. 3 shows that the maximal 10-min mean wind speed and 10-min mean wind direction

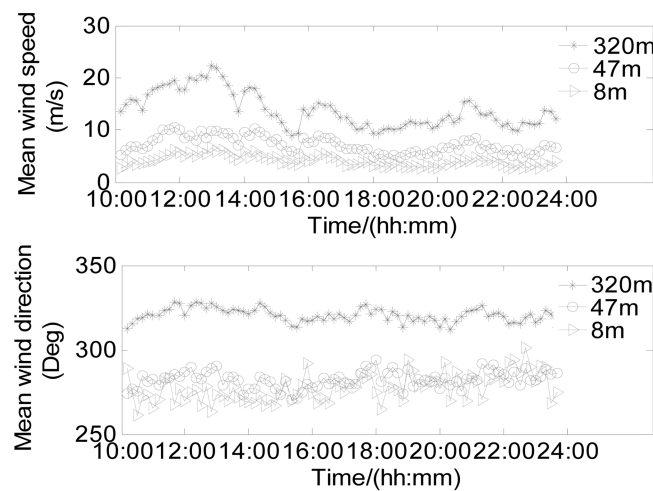


Fig. 3 Mean wind speed and mean wind direction distributions (windstorm “0320”)

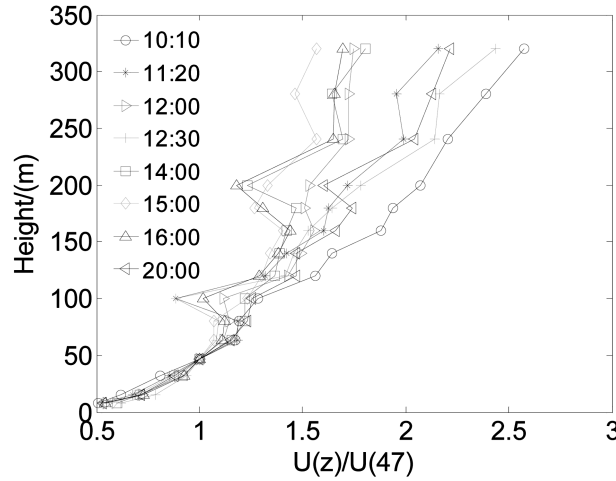


Fig. 4 10 min Mean wind speed profiles for the windstorm “0320”

measured at 320 m height during the windstorm was 22.3 m/s and varied in range of 312~328°, respectively. Shown in Fig. 4 are the 10-min mean wind speed profiles. It can be seen that most profiles exhibited “kinks” at 100 m or 200 m height, which could possibly be attributed to the influence of the changes in surface roughness from suburban terrain to urban terrain.

5. Evaluation of roughness length and zero-plane displacement

The roughness length (z_0) and zero-plane displacement (z_d) are two important parameters for describing the characteristics of atmospheric boundary layer. Accurate knowledge of these parameters is vital to describe and model the behavior of winds and turbulence in urban area. There are two classes of approach to estimating roughness length and zero-plane displacement in atmospheric boundary layer, as reviewed by Grimmond, *et al.* (1998), Grimmond and Oke (1999). One is called morph metric (or geometric) methods which use algorithms that relate aerodynamic parameters to measures of surface morphometry. The other is called micrometeorological (or anemometric) methods which use field observations of wind data to determine aerodynamic parameters included in theoretical relations derived from the logarithmic wind profile. The advantages and disadvantages of these methods have been described in detail in their review. In this study, the second method based on the measured wind profiles under neutral conditions is chosen to determine z_0 and d (Wieringa 1993, Takagi, *et al.* 2003). The logarithmic measurement height $\ln(z - z_d)$ in Eq. (2) is plotted against $U(z)$ at several heights by changing z_d , the value of z_d is taken when the maximum correlation between $\ln(z - z_d)$ and $U(z)$ is achieved. Once z_d is determined, then U_0^* and z_0 can be calculated from the slope and the intercept of the regression line, respectively.

To compute z_0 and z_d , the atmospheric stability of the air during the windstorm “0320” was delineated by the ratio of the height z to the Monin-Obukhov length:

$$z/L = -\frac{z \kappa \frac{g}{\theta} \overline{w\theta}}{U_0^{*3}} \quad (6)$$

where $\bar{\theta}$ is the mean temperature; g is the acceleration of gravity; $\overline{w\theta}$ is the surface heat flux. Fig. 5 presents variations of the stability parameter of the data recorded from the ultrasonic anemometer at 47 m height. It can be seen that the wind flow is neutral or near-neutral or unstable (negative) during the wind storm “0320”. However, if the zero-plane displacement (z_d) is taken into account, the absolute values of the stability parameter ($(z - z_d)/L$) become very small, indicating the flow is near-neutral or neutral ($(z - z_d)/L=0$) during the major period of the windstorm.

The data of the mean wind speed at lower measurement levels do not fit well to a logarithmic profile, especially below 32 m height, because the flow was strongly influenced by the surrounding buildings and trees. Meanwhile, it was observed that the measured mean wind speed profiles exhibit “kinks” at either 100 or 200 m height, below which the wind speed profile represents the terrain of the tower location while at higher levels the profile may be representative of the regional inhomogeneous terrain upwind of the roughness transition. Then, the data of the mean wind speed at heights of 32 m, 47 m, 63 m, 80 m under neutral condition were selected to evaluate the aerodynamic parameters for urban terrain. Average results of twenty samples with each containing 10-min recorded data, which were in good agreement with the logarithmic profile, were adopted for the present analysis.

In this study, the logarithmic measurement heights $\ln(z - z_d)$ in Eq. (2) is plotted against $U(z)$ at four heights by changing z_d from 0 m to 25 m at 0.1 m intervals. When the maximum correlation between $\ln(z - z_d)$ and $U(z)$ was achieved, the value of z_d was taken. Fig. 6 shows the roughness length (z_0) and zero-plane displacement (z_d) obtained from the mean wind speed profiles during the windstorm “0320” for northwesterly winds between 270° (west) and 290° . It can be observed that the profile-derived z_0 and z_d exhibit obvious variations during the windstorm. This may be attributed to several factors including that the effects of the wind speed. In addition, the average results of the surface roughness length and zero-plane displacement during the windstorm are listed in Table 2. For comparisons purposes, the values recommended by Wieringa (1993), and Grimmond and Oke (1999) for urban terrain are also given in the table. The recommended values of the roughness parameters for urban terrain were obtained based on the experimental studies over urban regions. It can be seen from the table that the results obtained in this study are in good agreement with the recommended values.

At the Beijing Meteorological Tower site, the surface friction velocity distributions based on the mean wind speed data are depicted in Fig. 7. Meanwhile, the friction velocity is also determined in terms of the turbulence components of longitudinal (u) and vertical (w) directions measured from the ultrasonic anemometer at 47 m height as:

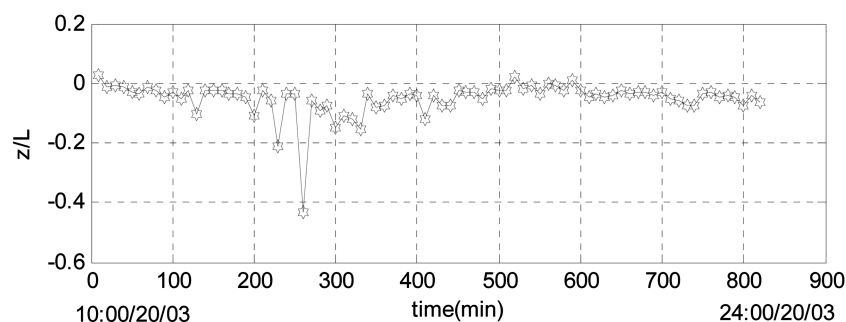


Fig. 5 Variation of the stability parameter at 47 m height

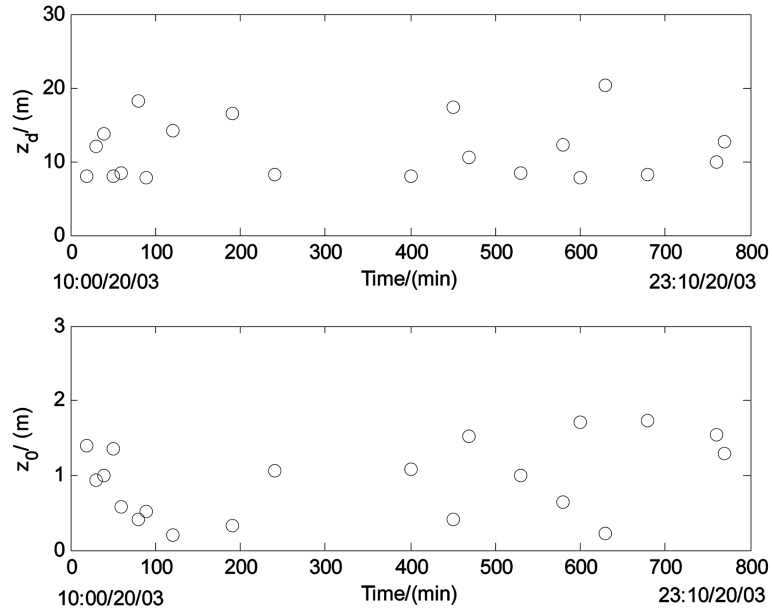


Fig. 6 Variations of the zero-displacement and roughness length

Table 2 Comparisons of average values of the parameters obtained from this study and those recommended by Wieringa (1993), and Grimmond and Oke (1999)

	z_0 (m)	z_d (m)
This study	1.0	11.6
Recommended values for urban terrain with a mixture of low residential houses and tall buildings	0.8~1.5	7~15

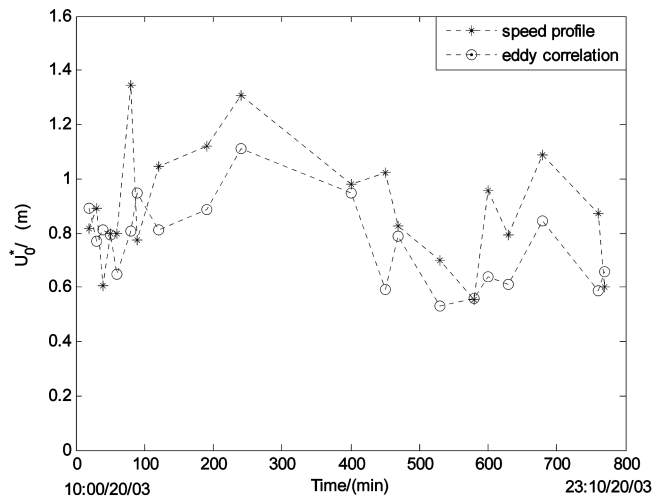


Fig. 7 Variation of the surface friction velocity obtained from velocity-profiles and the eddy correlation technique

$$U_0^* = \sqrt{-\overline{uw}} \quad (7)$$

The two methods provide comparable results for the data measured in neutral conditions. It is found that although the profile-derived friction velocities are slightly larger than those obtained by Eq.(7) called eddy-correlation technique, the variations of the surface friction velocities with time, obtained from the two methods, are similar.

6. Ground roughness exponent

The ground roughness exponent is an important parameter for the assessment of wind loads on structures. Fig. 8 shows variations of the ground roughness exponent (α) with the mean wind speed at 47 m height. The exponent was determined using the power law based on the field measured data. The average ground roughness exponent is found to be 0.348 during the windstorm. In the Chinese National Load Code (GB50009-2001), the ground roughness exponent with a constant 0.22 is recommended for such an urban terrain. Obviously, the ground roughness exponent determined based on the data measured during the windstorm “0320” is larger than the recommended one. Meanwhile, there is a tendency that the ground roughness exponent decreases with increase of the mean wind speed.

7. Wind speed profile models

It is of interest to compare the empirical mean speed profiles with the measured profiles. Vertical profiles of wind speed measured during the windstorm “0320”, normalized with the wind speed at 47 m height, are plotted in Fig. 9. For comparisons purposes, three empirical mean speed profiles (Power-law, Log-law and the D-H models) based on the parameters stipulated in the Chinese National Load Code (GB50009-2001) are also presented. It can be seen that the measured mean wind speed profile basically agrees with that determined by the D-H model except at heights of

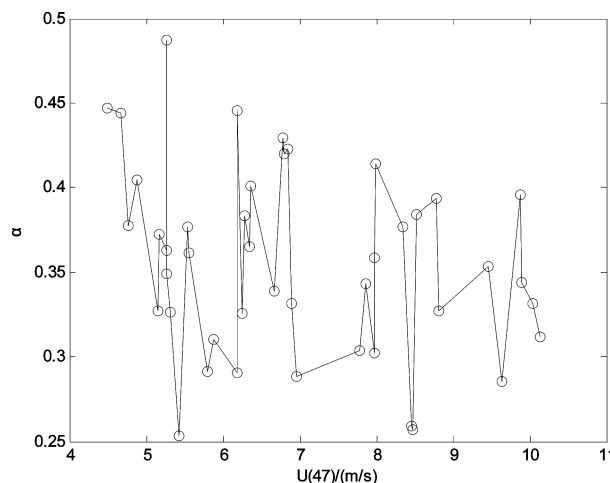


Fig. 8 Ground roughness exponent versus 10 min mean wind speed

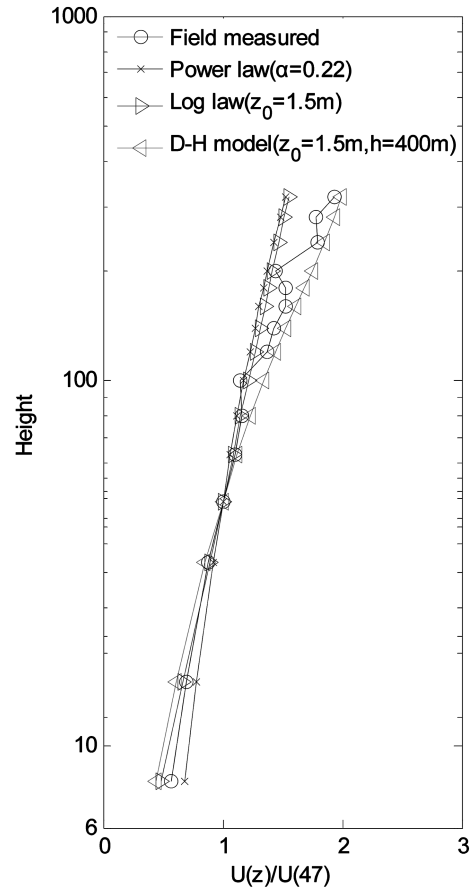


Fig. 9 Comparison of the measured wind speed profile averaged over 14 hours with those by the empirical models with adoption of the parameters stipulated by the Chinese National Load Code

100 m and 200 m. The profiles of the Power-law and Log-law models are also fit the measured data below 100m well; but at higher elevations above 100 m, the empirical models generally provide smaller predictions of wind speeds.

The heights of neutral ABL were calculated using Eq.(5) based on the D-H model, as shown in Fig. 10. It was found that the height of neutral ABL was nearly 2000m height when the wind speed reached to the maximum value during the windstorm. The average height of neutral ABL during the windstorm “0320” was found to be 1350 m, which exceeded appreciably the gradient height (400 m) as recommended by the Chinese National Load Code (GB50009-2001) for urban terrain.

Furthermore, the wind speed profiles based on the empirical models using the measured aerodynamic parameters (roughness length, zero-plane displacement and surface friction velocity) during the windstorm “0320” under neutral conditions are also obtained and compared with the measured profiles, which are plotted in Fig. 11. It is observed that the power-law profile is in closer agreement with the measured profile. The profile determined by the D-H model above 100 m is slightly smaller than the measured one. Even though the measured parameters were adopted, the log-law model underestimated the wind speeds above 100m height. Such a height is approximately equivalent to 10% of the ABL thickness, as discussed by Tieleman (2008).

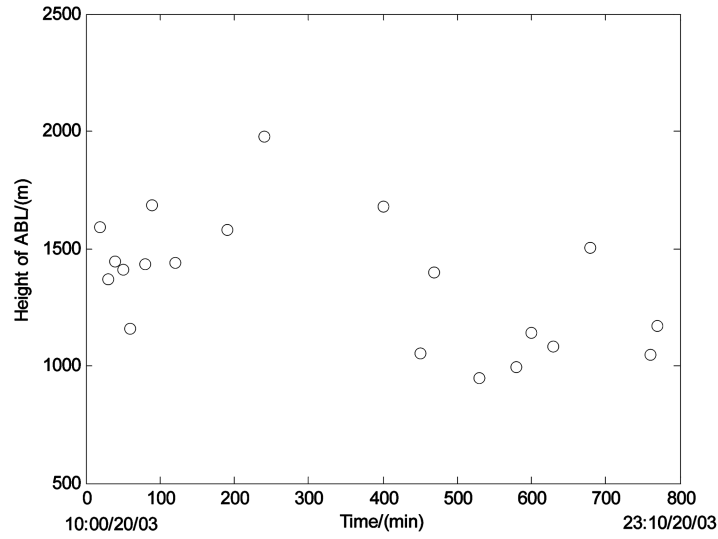


Fig. 10 Variation of the height of neutral ABL

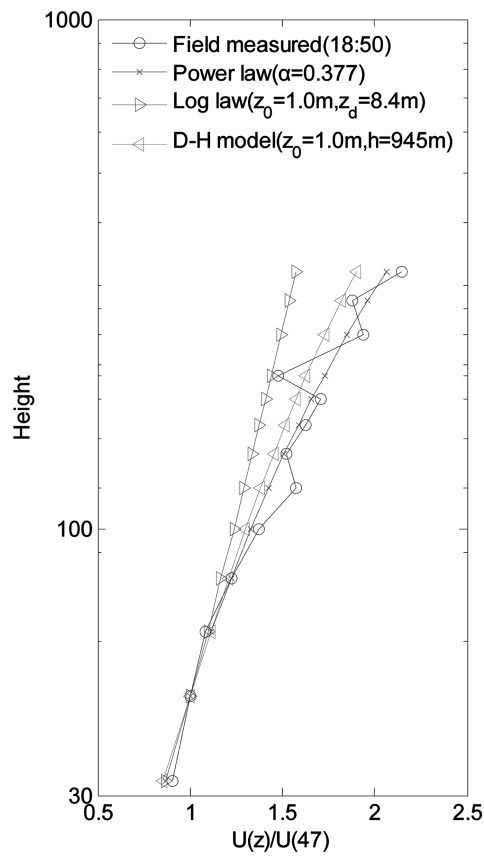


Fig. 11 Comparison of the measured 10 min mean speed profile with those by the empirical models with adoption of the measured parameters

8. Wind turbulence characteristics

8.1. Mean wind speed and direction

Fig. 12 shows the horizontal mean wind speed and wind direction averaged over 10 min, which were measured from the ultrasonic anemometer at 47 m height during the windstorms on February

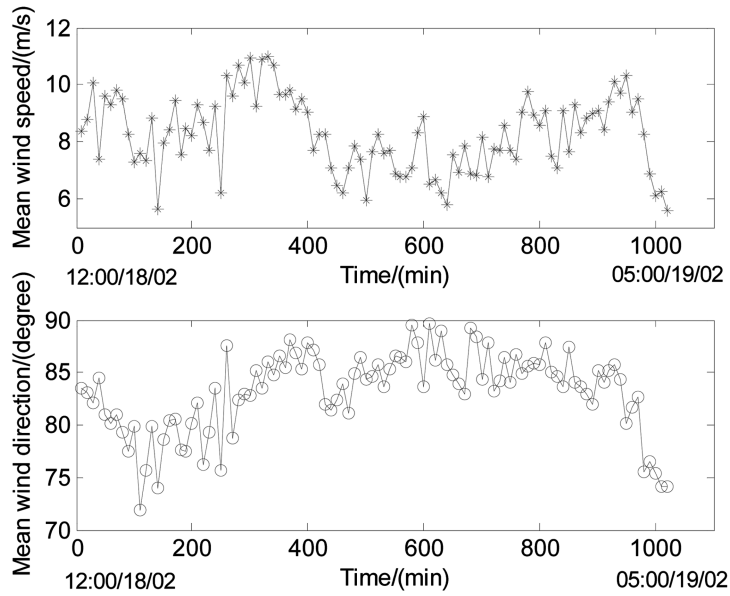


Fig. 12(a) 10 min averaged mean wind speed and wind direction during the windstorm “0218” ($z=47$ m)

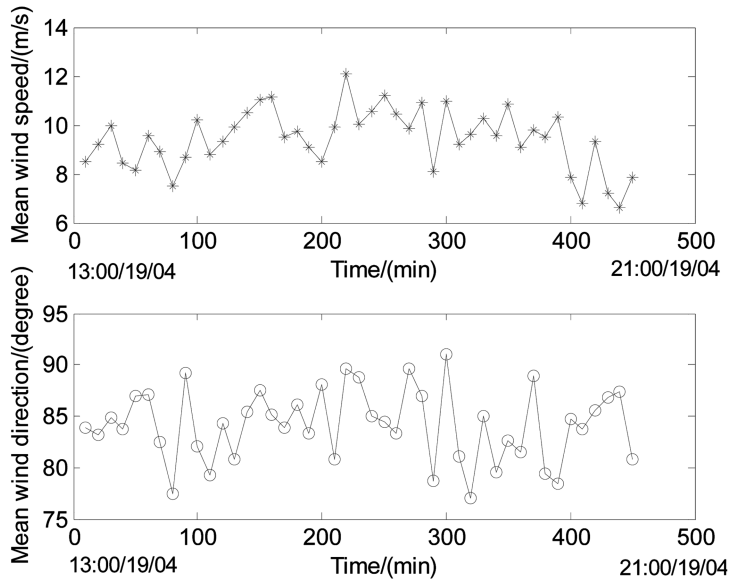


Fig. 12(b) 10 min averaged mean wind speed and wind direction during the windstorm “0419” ($z=47$ m)

18 (“0218”) and April 19 2003 (“0419”). The maximal 10-min mean wind speed recorded during the windstorms “0218” and “0419” were 11.0m/s and 12.1 m/s, respectively. The 10-min mean wind direction during the windstorms “0218” and “0419” varied in range of 72°~90° and 77°~91° with the mean wind direction of 83° and 84°, respectively. The results illustrate the mean wind direction relatively stabilized during the two windstorms.

8.2. Turbulence intensity and gust factor

The turbulence intensity and gust factor are two important parameters for describing the turbulence characteristics of wind flows. They can be calculated by the following equations.

$$I_i = \frac{\sigma_i}{U} \quad (i = u, v, w) \quad (8)$$

$$G_u(t_g) = 1 + \frac{\max(\overline{u(t_g)})}{U} \quad G_v(t_g) = 1 + \frac{\max(\overline{v(t_g)})}{U} \quad G_w(t_g) = 1 + \frac{\max(\overline{w(t_g)})}{U} \quad (9)$$

where U is the 10min mean wind speed; σ_i is the standard deviation of fluctuating wind speed component; t_g is gust duration (in this paper, $t_g=3$ s); $\max(\overline{u(t_g)})$, $\max(\overline{v(t_g)})$ and $\max(\overline{w(t_g)})$ are the largest mean wind speed over duration of t_g in longitudinal (u), lateral (v) and vertical (w) directions within 10 minutes, respectively.

Figs. 13 and 14 show variations of the three-dimensional turbulence intensity and gust factor with the horizontal mean wind speed measured from the ultrasonic anemometer at 47 m height during the windstorms “0218” and “0419”. It can be seen from the figures that the turbulence intensities in the three directions during the two windstorms decrease with the increase of the mean wind speed. The higher values of turbulence intensity for mean wind speed between 5 m/s and 6m/s may be due to the instability of the wind flow. At higher wind speeds the effect of stability decreases with turbulence intensity having lower values. The longitudinal gust factor decreases with the increase of the mean wind speed and approaches a constant when the wind speed becomes higher. However, the lateral and vertical gust factors remain almost unchanged regardless of the variation of the mean wind speed. The ratios for the gust factor among the three components determined from the measurements made during the windstorms “0218” and “0419” were 1:0.30:0.22 and 1:0.33:0.21, respectively. The average values of the turbulence intensity and gust factor in the longitudinal, lateral and vertical directions are similar for the data recorded from the two windstorms, as shown in Table 3. In the guidelines recommended by the Architectural Institute of Japan (AIJ-RLB-1996), the longitudinal turbulence intensity can be estimated by the empirical expression: $I_u=0.1(H/Z_G)^{-\alpha-0.5}$. As the height of the anemometer location is about 47 m from the ground, the calculated value of the longitudinal turbulence intensity from this equation is 0.286, while the values measured in the windstorms “0218” and “0419” were 0.289 and 0.314, respectively. Although both the measured values of the longitudinal turbulence intensity are slightly larger than the predicted one, the empirical formula is applicable for engineering practice. The average ratios of the turbulence intensity among the three directions obtained during the windstorms “0218” and “0419” are $I_u:I_v:I_w=1:0.78:0.59$ and $I_u:I_v:I_w=1:0.78:0.56$, respectively. The measured results are in good agreement with that ($I_u:I_v:I_w=1:0.75:0.50$) suggested by Solari and Piccardo (2001).

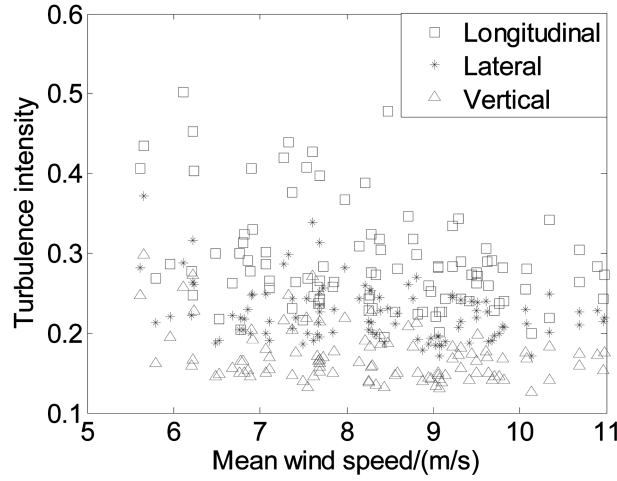


Fig. 13(a) Turbulence intensity versus 10 min mean wind speed (“0218”) $z=47$ m

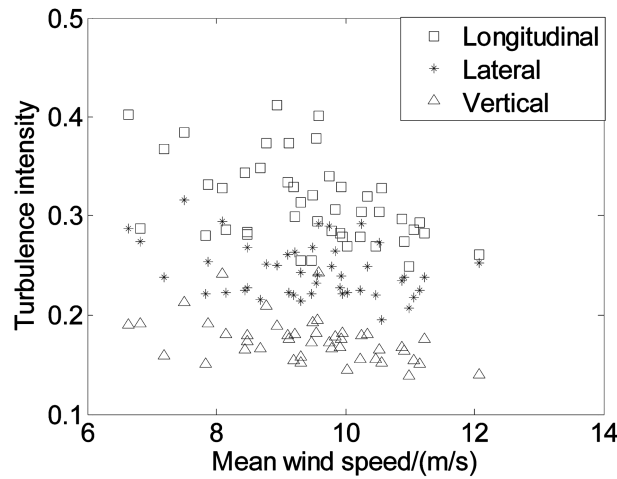


Fig. 13(b) Turbulence intensity versus 10 min mean wind speed (“0419”) $z=47$ m

8.3. Turbulence integral length scale

The turbulence integral length scale is another important parameter for describing the turbulence characteristics of wind flows. It is well known that the turbulence integral length scales deviate greatly in the atmospheric boundary layer and the method of calculating it also significantly influences the results (Li and Melbourne 1999, Li, *et al.* 2003, 2004a, 2004b, 2005). In this study, the turbulence integral length scale is calculated by the following equation:

$$L_i^x = \frac{U}{\sigma_i} \int_0^\infty R(\tau) d\tau, (i = u, v, w) \tag{10}$$

where $R(\tau)$ is the auto correlation function of fluctuating wind speed in each direction, respectively.

Fig. 15 shows variations of the three-dimensional turbulence integral length scales with the

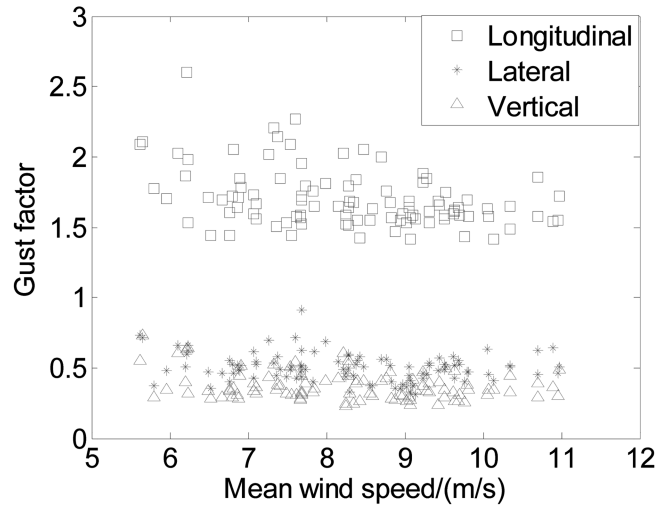


Fig. 14(a) Gust factor versus 10 min mean wind speed (“0218”) $z=47$ m

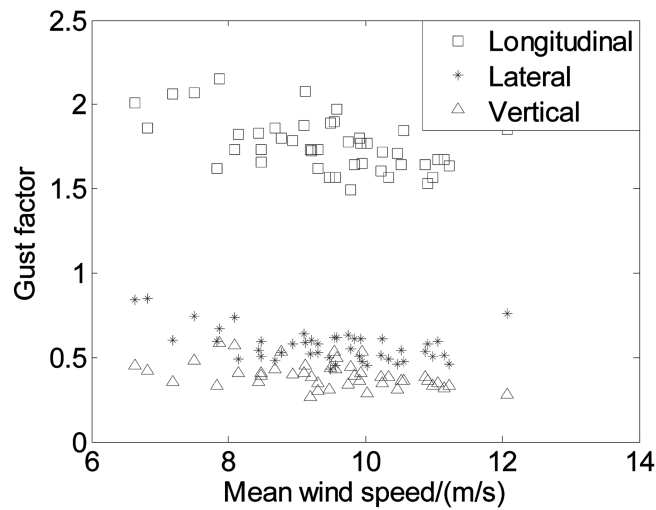


Fig. 14(b) Gust factor versus 10 min mean wind speed (“0419”) $z=47$ m

Table 3 Average values of the turbulence intensity and gust factor

Windstorms	Turbulence intensity			Gust factor		
	I_u	I_v	I_w	G_u	G_v	G_w
“0218”	0.289	0.255	0.171	1.701	0.504	0.371
“0419”	0.314	0.245	0.175	1.760	0.572	0.360

longitudinal mean wind speed measured at 47 m height during the windstorms “0218” and “0419”. It can be observed from the figure that there is a tendency for the turbulence integral length scales in the longitudinal and lateral directions to increase with the mean wind speed. However, the vertical

turbulence integral length scale is nearly invariant with the mean wind speed. The data listed in Table 4 indicate that the average vertical turbulence integral length scales measured during the two windstorms are similar, whereas there are noticeable differences between the averaged values of the longitudinal and lateral turbulence integral length scales determined from the two windstorms.

The average ratios of the turbulence integral length scale among the three directions measured during the windstorms “0218” and “0419” are $L_u^x : L_v^x : L_w^x = 1 : 0.43 : 0.18$ and, $L_u^x : L_v^x : L_w^x = 1 : 0.50 : 0.16$, respectively. It is evident that the average ratios of L_v^x / L_u^x and L_w^x / L_u^x obtained from the field measurements are larger than that ($L_u^x : L_v^x : L_w^x = 1 : 0.25 : 0.10$) suggested by Solari and Piccardo (2001). According to AIJ-RLB-1996, the longitudinal turbulence integral length scale can be estimated by the empirical expression: $L_u^x = 100(H/30)^{0.5}$. Such a value at the anemometer location estimated from this equation is 125 m. Although the measured average values of the

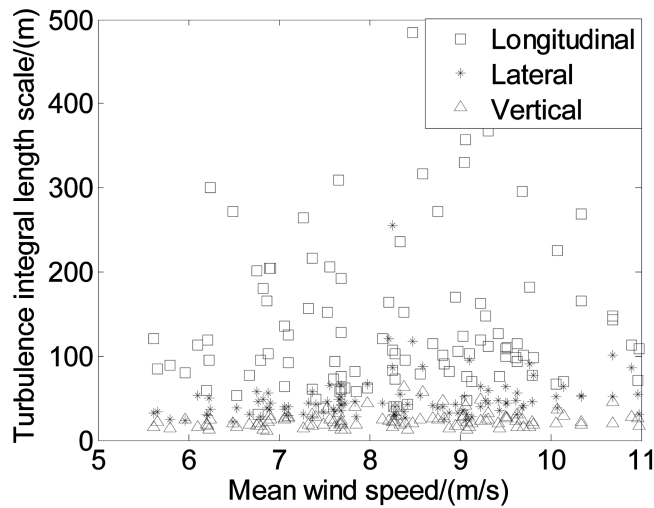


Fig. 15(a) Turbulence integral length scale versus 10 min mean wind speed (“0218”) $z=47$ m

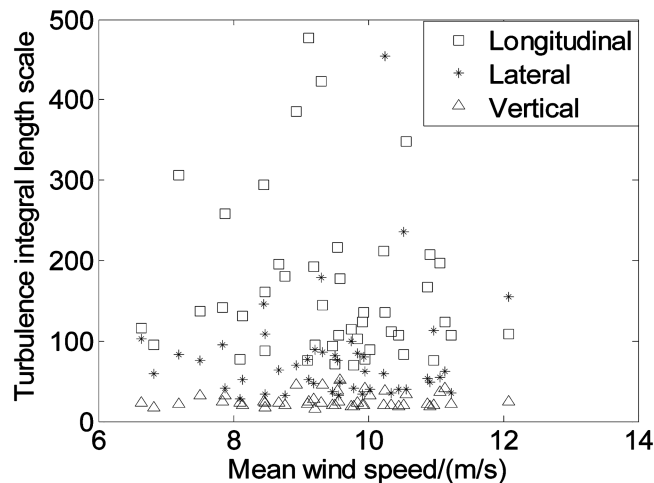


Fig. 15(b) Turbulence integral length scale versus 10 min wind mean speed (“0419”) $z=47$ m

Table 4 Average values of the turbulence integral length scale

Windstorms	$L_u^x(\text{m})$	$L_v^x(\text{m})$	$L_w^x(\text{m})$
“0218”	133	48	24
“0419”	163	81	26

longitudinal turbulence integral length scale (133 m and 163 m) are larger than the predicted one, the differences are acceptable in wind engineering applications. This suggests that the empirical equation recommended by AIJ-RLB-1996 is applicable in engineering practice.

8.4. Power spectral density and friction velocity

The energy distribution of fluctuating wind speed can be expressed in the form of power spectral density. The empirical expressions of power spectral densities are often described in the following equations (von Karman 1948, Panofsky and McCormick 1959, Davenport 1961, Kaimal, *et al.* 1972):

$$\frac{nS_u(n)}{\sigma_u^2} = \frac{4L_u^x n/U}{[1 + 70.7(L_u^x n/U)^2]^{5/6}} \quad \text{von Karman (Longitudinal)}$$

$$\frac{nS_i(n)}{\sigma_u^2} = \frac{4L_i^x n/U[1 + 755.2(L_i^x n/U)^2]}{[1 + 283.2(L_i^x n/U)^2]^{11/6}}, i = v, w; \quad \text{von Karman (Lateral and Vertical)}$$

$$\frac{nS_u(n)}{U^{*2}} = \frac{4x^2}{[1 + x^2]^{4/3}} \quad x = \frac{1200n}{U(10)} \quad \text{Davenport (Longitudinal)}$$

$$\frac{nS_v(n)}{U^{*2}} = \frac{15f}{(1 + 9.5f)^{5/3}} \quad f = \frac{nz}{U} \quad \text{Kaimal (Lateral)}$$

$$\frac{nS_w(n)}{U^{*2}} = \frac{6f}{(1 + 4f)^2} \quad f = \frac{nz}{U} \quad \text{Panofsky (Vertical)} \quad (11)$$

where n is frequency; z is the height of the anemometer location; $U(10)$ is the mean wind speed at 10 m height from the ground; U^* is friction velocity.

Figs. 16~18 show the normalized power spectral density estimates of fluctuating wind speed in the three directions, which were obtained based on the measured wind speed data at 47 m height with a relatively long sampling period (one hour). The empirical spectral models described in Eq.(11) are also plotted in these figures for comparison purposes. It can be seen from these figures that Davenport spectral model decreases too rapidly in the low-frequency range compared with the field measured spectra in the longitudinal direction. There are also some differences between the Kaimal spectral model and those from the field measurements at low frequencies. On the other hand, obvious differences between the Panofsky spectral model and the measured spectra are observed at high frequencies. However, the von Karman spectra are found to be in good agreement with the measured power spectral densities in the longitudinal, lateral and vertical directions, as shown in the three figures. This suggests that the von Karman-type spectra are able to describe the

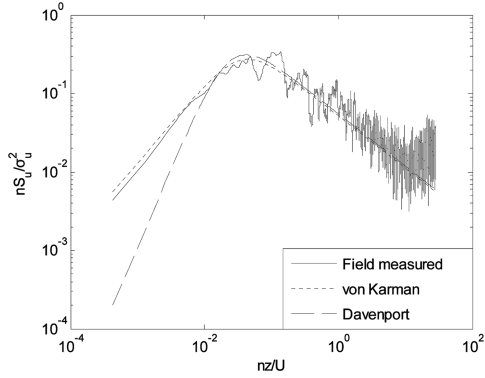


Fig. 16(a) Power spectral density of longitudinal wind speed for the data measured between 12:00 and 13:00 during the windstorm “0218” ($z=47$ m)

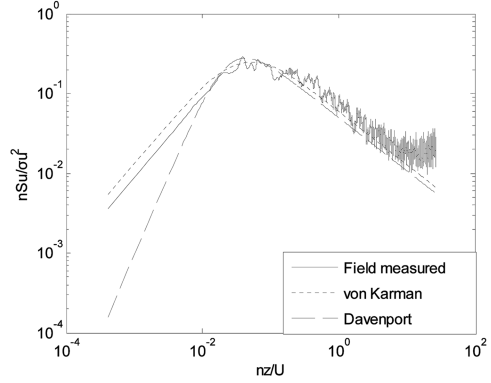


Fig. 16(b) Power spectral density of longitudinal wind speed for the data measured between 13:00 and 14:00 during the windstorm “0419” ($z=47$ m)

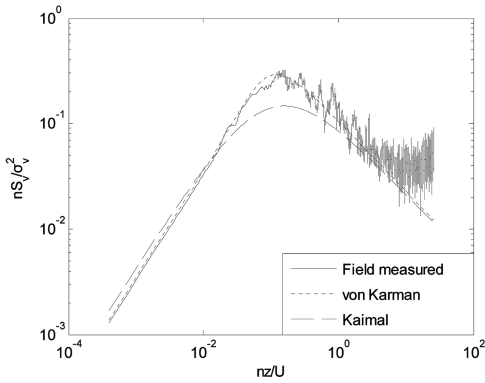


Fig. 17(a) Power spectral density of lateral wind speed for the data measured between 12:00 and 13:00 during the windstorm “0218” ($z=47$ m)

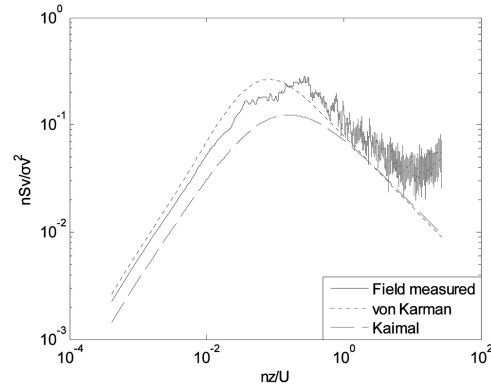


Fig. 17(b) Power spectral density of lateral wind speed for the data measured between 13:00 and 14:00 during the windstorm “0419” ($z=47$ m)

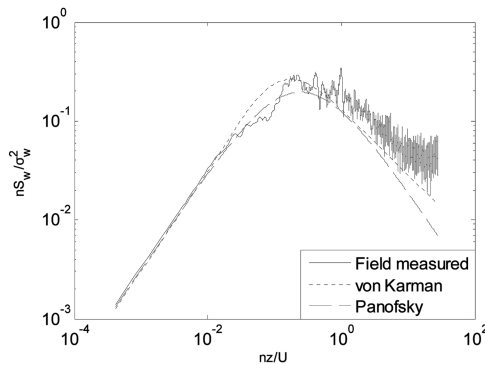


Fig. 18(a) Power spectral density of vertical wind speed for the data measured between 12:00 and 13:00 for the windstorm “0218” ($z=47$ m)

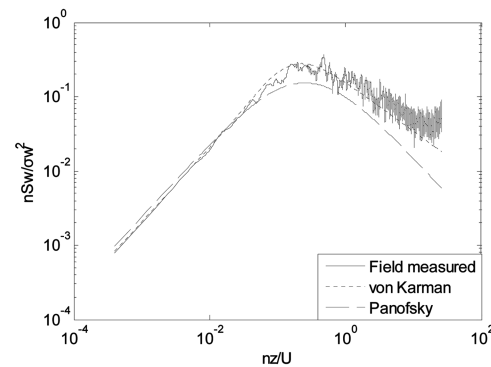


Fig. 18(b) Power spectral density of vertical wind speed for the data measured between 13:00 and 14:00 during the windstorm “0419” ($z=47$ m)

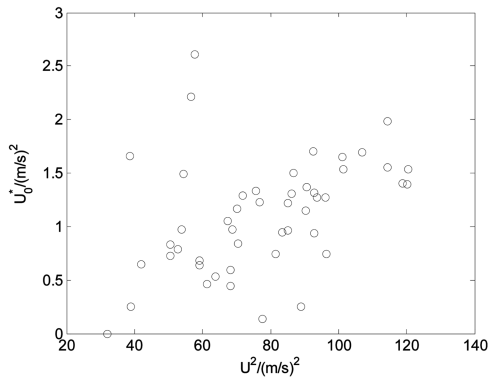


Fig. 19(a) The friction velocity versus 10 min mean wind speed during the windstorm “0218” ($z=47$ m)

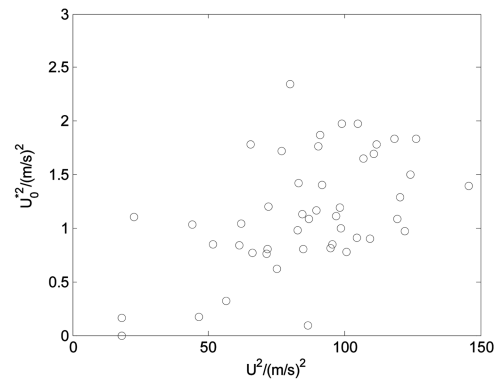


Fig. 19(b) The friction velocity versus 10 min mean wind speed during the windstorm “0419” ($z=47$ m)

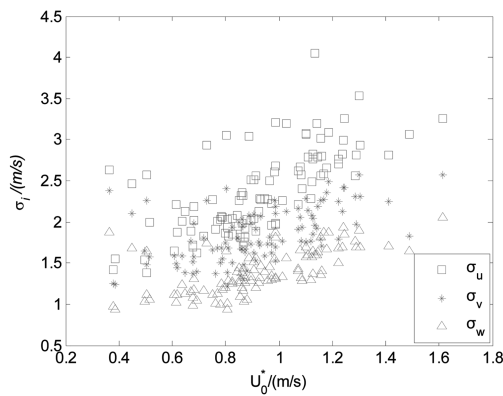


Fig. 20(a) Standard deviations of the fluctuating speed versus friction velocity (“0218”) ($z=47$ m)

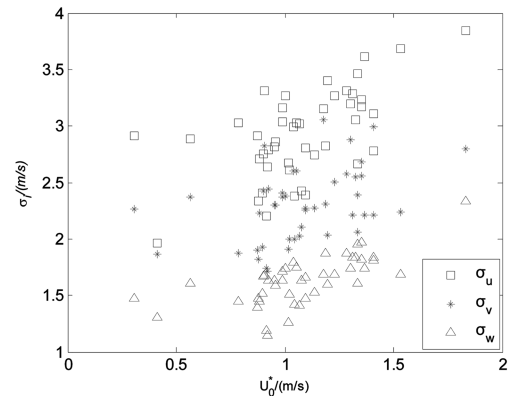


Fig. 20(b) Standard deviations of the fluctuating speed versus friction velocity (“0419”) ($z=47$ m)

energy distribution fairly well for the three components of wind speed above an urban terrain.

The friction velocity is one of the important aerodynamic parameters and generally varies with wind speed. The relationship between the friction velocity with the longitudinal mean wind speed is shown in Figs.19(a) and 19(b). It is observed from the figures that the friction velocity determined based on the measured data at 47 m height during the windstorm “0419” generally increases with the mean wind speed. Figs. 20(a) and 20(b) show variations of the standard deviations of the fluctuating wind speed with the longitudinal friction velocity measured at 47 m height during the two windstorms. The standard deviations of the fluctuating wind speed in the longitudinal, lateral and vertical directions all increase with the friction velocity.

9. Conclusion

This paper presents selected results recorded from the 325 m Beijing Meteorological Tower during several windstorms in Beijing in 2002 and 2003. Detailed analysis of the measured data was

conducted to investigate the wind speed profiles in the atmospheric boundary layer and turbulence characteristics of three-dimensional fluctuating wind speeds near ground over a typical urban area. Some conclusions from this study are summarized as follows:

- (1) The majority of the wind speed profiles exhibited “kinks” at 100 m and 200 m heights, which could possibly be caused by the changes in surface roughness from suburban terrain to urban terrain.
- (2) The profile-derived roughness length and zero-plane displacement under neutral flow conditions exhibited obvious variations during windstorms. The measured values agreed with those recommended by Wieringa (1993), Grimmond and Oke (1999). In addition, the variations of surface friction velocity with time, obtained from the measured wind profiles and the eddy-correlation technique, were similar.
- (3) The measured average ground roughness exponent was 0.348 which is larger than that stipulated by the Chinese National Load Code. The measured values of the ground roughness exponent were found to decrease with the increase of the mean wind speed.
- (4) The average height of neutral ABL, which was obtained by Eq.(5) based on the data measured during the windstorm “0320”, was found to be 1350 m which exceeded appreciably the gradient height (400 m) as recommended by the Chinese National Load Code (GB50009-2001) for urban terrain.
- (5) The turbulence intensities in the three directions during the windstorms “0218” and “0419” all decreased with the increase of the mean wind speed. The measured average longitudinal turbulence intensity values were in good agreement with that determined by AIJ-1996. The average ratios of the turbulence intensity among the three directions obtained during the windstorms “0218” and “0419” were $I_u : I_v : I_w = 1 : 0.78 : 0.59$ and $I_u : I_v : I_w = 1 : 0.78 : 0.56$, respectively; while such ratios for the gust factor among the three components were 1:0.30:0.22 and 1:0.33:0.21.
- (6) There was a tendency for the turbulence integral length scale values in the longitudinal and lateral directions to increase with the increase of the mean wind speed. The average ratios of the turbulence integral length scale among the three directions measured during the windstorms “0218” and “0419” were $L_u^x : L_v^x : L_w^x = 1 : 0.43 : 0.18$ and $L_u^x : L_v^x : L_w^x = 1 : 0.50 : 0.16$, respectively. The comparative study between the measured longitudinal turbulence integral length scales and that estimated by AIJ-1996 indicated that the empirical formula recommended by AIJ is applicable to engineering practice.
- (7) The measured power spectral densities of fluctuating wind speed in the longitudinal, lateral and vertical directions were in good agreement with the von Karman-type spectra, suggesting that the von Karman-type spectra can describe the energy distribution fairly well for the three wind velocity components over a typical urban area.
- (8) The friction velocity values obtained based on the field measurements were found to increase with the mean wind speed. The standard deviations of fluctuating wind velocities in the longitudinal, lateral and vertical directions also increased with the surface friction velocity.

Acknowledgements

The work described in this paper was supported by a research grant from the Research Committee of City University of Hong Kong (Project No. 7002205). The authors wish to acknowledge the joint efforts of all members of State Key Lab. of Atmospheric Boundary Layer Physics and Atmospheric Chemistry, Institute of Atmospheric Physics, Chinese Academy of Sciences, Beijing.

References

- AII-RLB-1996 (1996), *Recommendations for loads on buildings*, Architecture Institute of Japan, (English version, 1996).
- Al-Jiboori, M.H. and Hu, F. (2005), "Surface roughness around a 325-m meteorological tower and its effect on urban turbulence", *Adv. Atmos. Sci.*, **22**(4), 595-605.
- ASCE 7-02 (2002), *American Society of Civil Engineers Minimum Design Loads for Buildings and Other Structures*, ASCE, New York.
- Baklanov, A.A. and Joffre, S.M. (2008), "The effect of stratification on the aerodynamic roughness length and displacement height", *Bound.-Lay. Meteorol.*, **129**, 179-190.
- Carl, M.D., Tarbell, T.C. and Panofsky, H.A. (1973), "Profiles of wind and temperature from towers over homogeneous terrain", *J. Atmos. Sci.*, **30**, 788-794.
- Cheng, C.H., Wu, J.C., Wang, J. and Lin, Y.Y. (2007), "Wind characteristics of typhoon and monsoon", *Proc. of The Twelfth Int. Conf. on Wind Engineering*, July 1st-6th, Cairns, Australia, 711-717.
- Cook, N.J. (1997), "The Deaves and Harris ABL model applied to heterogeneous terrain", *J. Wind Eng. Ind. Aerod.*, **66**, 197-214.
- Davenport, A.G. (1960), "Rationale for determining design wind velocities", *J. Struct. Eng. ASCE*, **86**, 39-68.
- Davenport, A.G. (1961), "The spectrum of horizontal gustiness near the ground in high winds", *Q. J. Roy. Meteor. Soc.*, **87**, 194-211.
- Deaves, D.M. (1981a), "Computations of wind flow over changes in surface roughness", *J. Wind Eng. Ind. Aerod.*, **7**, 65-94.
- Deaves, D.M. (1981b), "Terrain dependence of longitudinal R. M. S. velocities in the neutral atmosphere", *J. Wind Eng. Ind. Aerod.*, **8**, 259-274.
- Eliasson, I., Offerle, B., Grimmond, C.S.B. and Lindqvist, S. (2006), "Wind fields and turbulence statistics in an urban street canyon", *Atmos. Environ.*, **40**, 1-16.
- GB50009-2001 (2002), *Load code for the design of building structures*, China Architecture & Building Press, Beijing.
- Grag, R.K., Lou, J.X. and Kasperski, M. (1997), "Some features of modeling spectral characteristics of flow in boundary layer wind tunnels", *J. Wind Eng. Ind. Aerod.*, **72**, 1-12.
- Grant, A.L.M. (1994), "Wind profiles in the stable boundary layer, and the effect of low relief", *Q. J. Roy. Meteor. Soc.*, **120**, 27-46.
- Grimmond, C.S.B., King, T.S., Roth, M. and Oke, T.R. (1998), "Aerodynamic roughness of urban areas derived from wind observations", *Bound.-Lay. Meteorol.*, **89**, 1-24.
- Grimmond, C.S.B. and Oke, T.R. (1999), "Aerodynamic properties of urban areas derived from analysis of surface form", *J. Appl. Meteorol.*, **38**, 1262-1292.
- Holmes, J.D., Banks, R.W. and Paevere, P. (1997), "Measurements of topographic multipliers and flow separation from a steep escarpment. Part I. Full scale measurements", *J. Wind Eng. Ind. Aerod.*, **69-71**, 885-892.
- Holmes, J.D., Baker, C.J., English, E.C. and Choi, E.C.C. (2005), "Wind structure and codification", *Wind Struct.*, **8**(4), 235-250.
- Holmes, J.D. (2007), *Wind loading of structures*, Taylor & Francis, New York.
- Holtslag, A.A.M. (1984), "Estimates of diabatic wind speed profiles from near surface weather observations", *Bound.-Lay. Meteorol.*, **29**, 225-250.
- Kaimal, J.C., Wyngaard, J.C., Izumi, Y. and Cote, O.R. (1972), "Spectral characteristics of surface-layer turbulence", *Q. J. Roy. Meteor. Soc.*, **98**, 563-589.
- Karlsson, S. (1986), "The Applicability of Wind Profile Formulas to an Urban-Rural Interface Site", *Bound.-Lay. Meteorol.*, **34**, 333-355.
- Korrell, A., Panofsky, H.A. and Rossi, R.J. (1982), "Wind profiles at the Boulder tower", *Bound.-Lay. Meteorol.*, **22**, 295-312.
- Law, S.S., Bu, J.Q., Zhu, X.Q. and Chan, S.L. (2006), "Wind characteristics of Typhoon Dujuan as measured at a 50 m guyed mast", *Wind Struct.*, **9**(5), 387-396.
- Li, Q.S. and Melbourne, W.H. (1999), "The effects of large scale turbulence on pressure fluctuations in separated and reattaching flows", *J. Wind Eng. Ind. Aerod.*, **83**, 159-169.

- Li, Q.S., Xiao, Y.Q., Wong, C.K. and Jeary, A.P. (2003), "Field measurements of wind effects on the tallest building in Hong Kong", *Struct. Des. Tall Spec.*, **12**, 67-82.
- Li, Q.S., Xiao, Y.Q., Wong, C.K. and Jeary, A.P. (2004a), "Field measurements of typhoon effects on a super tall building", *Eng. Struct.*, **26**, 233-244.
- Li, Q.S., Wu, J.R., Liang, S.G., Xiao, Y.Q. and Wong, C.K. (2004b), "Full-scale measurements and numerical evaluation of wind-induced vibration of a 63-story reinforced concrete super tall building", *Eng. Struct.*, **26**, 1779-1794.
- Li, Q.S., Xiao, Y.Q. and Wong, C.K. (2005), "Full-scale monitoring of typhoon effects on super tall buildings", *J. Fluids Struct.*, **20**, 697-717.
- Olesen, H.R., Larsen, S.E. and Hojstrup, J. (1984), "Modeling velocity spectra in the tower part of the planetary boundary layer", *Bound.-Lay. Meteorol.*, **29**, 285-312.
- Panofsky, H.A. and McCormik, R.A. (1959), *The spectrum of vertical velocity near the surface, Collection of Mineral industries*, Pennsylvania University, University Park.
- Panofsky, H.A. and Petersen, E.L. (1972), "Wind profiles and change of terrain roughness at Riso", *Q. J. Roy. Meteor. Soc.*, **98**, 845-854.
- Panofsky, H.A., Tennekes, H., Lenschow, D.H. and Wyngaard, J.C. (1977), "The characteristics of turbulent velocity components in the surface layer under convective conditions", *Bound.-Lay. Meteorol.*, **11**, 355-361.
- Panofsky, H.A., Larko, D., Lipschutz, R., Stone, G., Bradley, E.F., Bowen, A.J. and Hojstrup, J. (1982), "Spectra of velocity components over complex terrain", *Q. J. Roy. Meteor. Soc.*, **108**, 215-230.
- Roth, M. (2000), "Review of atmospheric turbulence over cities", *Q. J. Roy. Meteor. Soc.*, **126**, 941-990.
- Schroeder, J.L., Edwards, B.P. and Giammanco, I.M. (2009), "Observed tropical cyclone wind flow characteristics", *Wind Struct.*, **12**(4), 347-379.
- Shiau, B.S. and Chen, B.Y. (2002), "Observation on wind turbulence characteristics and velocity spectra near the ground at the coastal region", *J. Wind Eng. Ind. Aerod.*, **90**, 1671-1681.
- Simiu, E. and Scanlan, R.H. (1996), *Wind effects on structures-fundamentals and applications to design*, John Wiley & Sons, Inc., 42-43.
- Solari, G. and Piccardo, G. (2001), "Probabilistic 3-D turbulence modeling for gust buffeting of structures", *Probabilist. Eng. Mech.*, **16**, 73-86.
- Takagi, K., Miyata, A., Harazono, Y., Ota, N., Komine, M. and Yoshimoto, M. (2003), "An alternative approach to determining zero-plane displacement, and its application to a lotus paddy field", *Agr. Forest Meteorol.*, **115**, 173-181.
- Tamura, Y., Suda, K., Sasaki, A., Iwatani, Y., Fujii, K., Ishibashi, R. and Hibi, K., (2001), "Simultaneous measurements of wind speed profiles at two sites using Doppler sodars", *J. Wind Eng. Ind. Aerod.*, **89**, 325-335.
- Tamura, Y., Iwatani, Y., Hibi, K., Suda, K., Nakamura, O., Maruyama, T. and Ishibashi, R., (2007), "Profiles of mean wind speeds and vertical turbulence intensities measured at seashore and two inland sites using Doppler sodars", *J. Wind Eng. Ind. Aerod.*, **95**, 411-427.
- Thomas, R. and Vogt, S. (1993), "Variances of the vertical and horizontal wind measured by tower instruments and sodar", *Appl. Phys. B-Lasers O.*, **57**, 19-26.
- Thuillier, R.H. and Lappe, V.O. (1964), "Wind and temperature profile characteristics from observations on a 1400 ft tower", *J. Appl. Meteorol.*, **3**, 299-306.
- Tieleman, H.W. (2008), "Strong wind observations in the atmospheric surface layer", *J. Wind Eng. Ind. Aerod.*, **96**, 41-77.
- Vogt, S. and Thomas, P. (1995), "Sodar-a useful remote sounder to measure wind and turbulence", *J. Wind Eng. Ind. Aerod.*, **54-55**, 163-172.
- von Karman, T. (1948), "Progress in the statistical theory of turbulence", *Proc. of the National Academy of Sciences*, **34**, 530-539.
- Wieinga, J. (1993), "Representative roughness parameters for homogeneous terrain", *Meteorology*, **63**, 323-363.
- William, P.K. and Wilfried, B. (1986), "Wind profile constants in a neutral atmospheric boundary layer over layer over complex terrain", *Bound.-Lay. Meteorol.*, **34**, 35-54.
- Zilitinkevich, S.S., Mammarella, I., Baklanov, A.A. and Joffre, S.M. (2008), "The effect of stratification on the aerodynamic roughness length and displacement height", *Bound.-Lay. Meteorol.*, **129**, 179-190.